CHAPTER 193

TIDAL STREAM FLOW SOLVED BY GALERKIN TECHNIQUE

By L. H. Smith & R. T. Cheng

Water Resources Division
U.S. Geological Survey

I. The Problem

The total discharges in a tidally influenced stream reach are known to be related to the stages (water levels) at the ends of the reach. The discharge-stage relationships can be derived from the conservation principles of mass and momentum under a few simplifying assumptions. Solutions of the governing equations with appropriate boundary and initial conditions give spatial and temporal variations of the flow in the reach. Practically, the most needed information are the instantaneous discharges, which, in many instances, provide guidance for water resources management decision making. Unfortunately, measuring the instantaneous discharge in a tidal reach is often difficult, tedious and costly. However, measuring the stages of a tidal reach is relatively simple, inexpensive and is done routinely. To determine discharges from measured water levels has been the subject of the present study.

The governing conservation equations of momentum and mass when written for unidirectional, constant density, transient flow are, respectively,

$$L_1(u,Z) = \frac{\partial u}{\partial t} + u\frac{\partial u}{\partial x} + g\frac{\partial Z}{\partial x} + G|u|u + (q/A)u = 0, \tag{1}$$

$$L_2(u,Z) = \frac{\partial Z}{\partial t} + u\frac{\partial Z}{\partial x} + (A/B)\frac{\partial u}{\partial x} + (S_o + \frac{\partial A}{\partial x}/B)u - (q/B) = 0, \tag{2}$$

where

A = channel cross-sectional area
B = width of channel cross-section at water surface
g = gravitational acceleration,
$G = gn^2/(1.49^2R^{4/3})$, n being Manning's coefficient,
q = lateral inflow per unit length of channel,
R = hydraulic radius of a cross-section,
S_o = slope of the channel bottom,
t = time,
u = average water velocity for cross-sectional area A,
x = direction of flow,
Z = elevation of water surface,

as indicated in Figure 1.

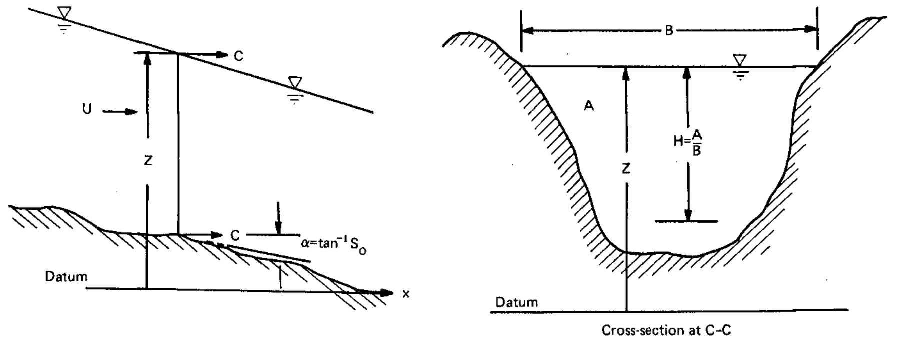

Figure 1. Schematic Diagram of a Tidal Reach

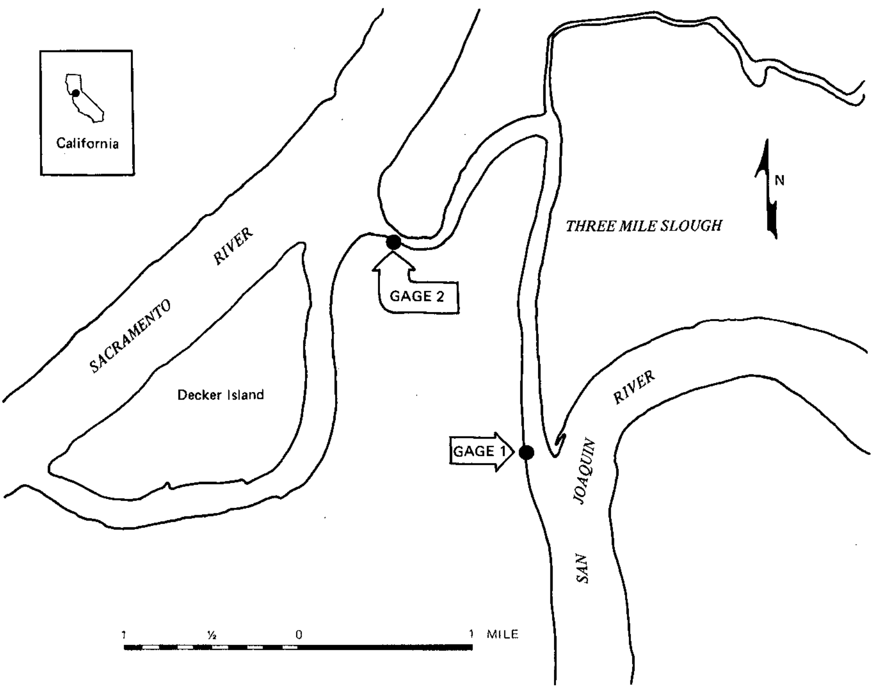

Figure 2. Plane View of Three-mile Slough, California

These equations assume that the flow is relatively uniform in any cross-section of the reach so that an average velocity u can be used to characterize the total discharge by Au. Though the cross-sectional area is treated as a variable, we further assume that A can be schematized by stacked trapezoids and that a linear representation of variation of A along the stream is sufficient. Stoker (1957), Chow (1959), Dronkers (1964) and Baltzer and Lai (1968) provide derivations and further discussion of these equations. The governing equations are coupled, nonlinear partial differential equations of hyperbolic type, which with specified water stages as the boundary conditions at ends of a channel segment, and initial conditions specified within the channel segment, form an initial-boundary value problem without known analytical solution.

Resorting to numerical techniques, Baltzer and Lai (1968) have considered the power series method, the implicit finite-difference method, and the method of characteristics to construct solutions of the discharges. Of these methods, the method of characteristics appears to produce the most accurate solutions. Recently, many classical variational techniques have attracted attention of researchers in relation to finite element methods, and use of the finite element methods in solid mechanics has been very fruitful.

Applications of the finite element techniques to hyperbolic equations are not yet numerous. Wang, et al. (1972) considered the one-dimensional primitive shallow water equation using cubic Hermite basis functions. Smith (1975) demonstrated that a Galerkin-finite element solution using linear basis functions compared favorably with those obtained by Baltzer and Lai (1968). Following a similar approach, a finite element solution of the Saint-Venant equation using linear basis functions was presented by Cooley and Moin (1976). They found that a stage boundary condition at each end of a channel segment must be implemented with the aid of the characteristic equations.

In this study we illustrate the use of cubic Hermite polynomials as basis functions in formulating a Galerkin-finite element solution to Eqs. (1) and (2). We explore the use of explicit and implicit time-differencing schemes. For a field case we compare measured discharges with discharges computed by the solution algorithm using measured stages as boundary values.

II. Galerkin-Finite Element Method

A. Galerkin Procedure

A general way to construct a finite element solution to a set of partial differential equations (such as (1) and (2)) is to employ the method of weighted residuals (Finlayson, 1972). For an M-th order approximate solution $\bar{u}$ and $\bar{Z}$ for the dependent variables u and Z, we write

$$\bar{u}(x,t) = \sum_{i=1}^{M} a_i(t)\psi_i(x), \text{ and} \tag{3}$$

$$\bar{Z}(x,t) = \sum_{i=1}^{M} b_i(t)\psi_i(x), \tag{4}$$

where ψ_i, i=1,2,..., M are a carefully selected family of linearly independent functions called basis functions. If residual functions R_1 and R_2 are defined as

$$R_1(x,t) = L_1(\bar{u},\bar{Z}), \text{ and}$$
$$R_2(x,t) = L_2(\bar{u},\bar{Z}),$$

the method of weighted residuals obtains $\bar{u}$ and $\bar{Z}$ by making integrals of the residuals R_1 and R_2 vanish over the entire domain of interest with respect to certain weighting functions W_i, i=1,2,..., M. In other words,

$$\int_o^L R_1(x,t)W_i(x)dx = o, \text{ and} \tag{5}$$
$$\int_o^L R_2(x,t)W_i(x)dx = o, \tag{6}$$

for i=1,2,...M, where L is the length of the entire channel segment of interest. When the weighting functions are defined and the integrals are evaluated, Eqs. (5) and (6) become a system of 2M simultaneous, ordinary differential equations of a_i's and b_i's, i=1,2,...,M. The Galerkin procedure assumes that $W_i = \psi_i$, and the classical Galerkin procedure is equivalent to the scheme of eigenfunction expansion for solution of boundary value problems. In finite element applications the basis functions ψ_i are neither complete nor orthogonal, so that the Galerkin procedure only implies that the weighted-averaged residuals are zero over the domain with respect to the basis functions.

Following the Galerkin procedure, and using Eqs. (1) - (4), Eqs. (5) and (6) can be written in matrix form as

$$[T]\frac{d\{a\}}{dt} + \left[P(\underline{a})\right]\{a\} + g\left[S\right]\{b\} + \left[Q(G|u| + q/A)\right]\{a\} = 0, \tag{7}$$

$$[T]\frac{d\{b\}}{dt} + \left[P(\underline{a})\right]\{b\} + \left[P(A/B)\right]\{a\} + \left[Q(S_o + \frac{\partial A}{\partial x}/B)\right]\{a\} - [T]\{q/B\} = 0, \tag{8}$$

where

{ }= a column vector of dimension M,

$$[T] = \int_o^L \psi_i\psi_j dx, \tag{9}$$
$$[S] = \int_o^L \psi_i\frac{\partial\psi_j}{\partial x} dx, \text{ and} \tag{10}$$
$$\left[P(\underline{f})\right] = \sum_{k=1}^{M} f_k U_{ijk}, \tag{11}$$
$$\left[Q(f)\right] = \sum_{k=1}^{M} f_k V_{ijk} \tag{12}$$

in which

$$U_{ijk} = \int_0^L \psi_i \frac{\partial\psi_j}{\partial x} \psi_k dx, \tag{13}$$

$$V_{ijk} = \int_0^L \psi_i \psi_j \psi_k dx, \text{ and} \tag{14}$$

for a given function f(x) we write

$$f(x) = \sum_{k=1}^{m} f_k \psi_k(x). \tag{15}$$

Calculations for f_k are straightforward and clear when defined in terms of $\psi_k(x)$. Appendix I gives expressions for the above integrals in which $\psi_k(x)$ are cubic Hermite polynomials. In terms of local coordinates, the integrals defining the coefficient matrices have been evaluated explicitly. Appendix II contains specific entries for these matrices.

Application of the Galerkin-finite element procedure to the conservation equations produces the 2M - coupled, nonlinear, ordinary differential equations, Eqs. (7) and (8). In this study both the explicit and implicit finite-difference schemes have been used in the temporal space.

B. Explicit Time-differencing

Of the explicit time-differencing schemes, predictor-corrector schemes are well-suited for solving Eqs. (7) and (8). A fourth order Haming's modified predictor-corrector formula (Ralston and Wilf, 1960) has been employed in this study for which stages and discharges and their time-derivatives at three consecutive, equally-spaced times are used to predict their values at a fourth time. The time derivatives of the stages and discharges at the fourth time can thus be evaluated by Eqs. (7) and (8), and the processes repeated. A Runge-Kutta formula must be used up to the fourth time step to start the fourth order predictor-corrector. This integration scheme is explicit and requires relatively small time steps to maintain numerical stability. Because of its explicit nature, specification of stages at end boundaries must be implemented with the aid of characteristic equations (Cooley and Moin, 1976).

C. Implicit Time-differencing

Alternatively, in many applications an implicit Crank-Nicholson time differencing scheme which is numerically stable is preferred. Before applying a Crank-Nicholson scheme, we employ the quasi-linearization procedure to the governing equations, Eqs. (1) and (2).

1. Method of Quasi-linearization

As shown above the Galerkin procedure is general. When applied to nonlinear partial differential equations it only results in a system of nonlinear ordinary differential equations. The question of nonlinearity is dealt with by first linearizing the governing equations and introducing an iteration upon them. The Galerkin procedure is then applied to the linearized system to construct numerical solutions for each step of the iteration. This is plausible, and the following nonlinear terms are approximated by

$$u\frac{\partial u}{\partial x} \cong u^{(n)}\frac{\partial u^{(n+1)}}{\partial x} + u^{(n+1)}\frac{\partial u^{(n)}}{\partial x} - u^{(n)}\frac{\partial u^{(n)}}{\partial x} \tag{16}$$

$$u\frac{\partial Z}{\partial x} \cong u^{(n)}\frac{\partial Z^{(n+1)}}{\partial x} + u^{(n+1)}\frac{\partial Z^{(n)}}{\partial x} - u^{(n)}\frac{\partial Z^{(n)}}{\partial x} \tag{17}$$

where the superscript indicates the order of the iteration. When the (n + 1)-th order solutions are sought, the n-th order solutions are known functions. Thus, Eqs. (16) and (17) are linear with respect to the (n + 1)-th order solutions. Normally, the previous time solutions of u and Z are taken as the zeroth order solutions. It can be demonstrated that the quasi-linearization is but the extension of Newton's method to functional space. If convergence can be reached, the iteration converges at a quadratic rate (Bellman and Kalaba, 1965). Some nonlinearities in Eqs. (1) and (2) are weak and may be treated by a time delayed approximation. Thus Eqs. (1) and (2) become

$$\tilde{L}_1(u,Z) = \frac{\partial u}{\partial t} + u^{(n)}\frac{\partial u}{\partial x} + u\frac{\partial u^{(n)}}{\partial x} + g\frac{\partial Z}{\partial x} + G\,|u^{(o)}|\,u - u^{(n)}\frac{\partial u^{(n)}}{\partial x} + \left(q/A\right)u = 0, \tag{18}$$

$$\tilde{L}_2(u,Z) = \frac{\partial Z}{\partial t} + u^{(n)}\frac{\partial Z}{\partial x} + u\frac{\partial Z^{(n)}}{\partial x} + \left(\frac{A}{B}\right)^{(o)}\frac{\partial u}{\partial x} + \left[S_o + \frac{\partial A}{\partial x}/B\right]^{(o)}u - \left(q/B\right) = 0, \tag{19}$$

where $\tilde{L}_1$ and $\tilde{L}_2$ are linear operators in which the superscript (n + 1) is dropped for clarity, and terms with superscript (o) are treated with the time-delayed approximation.

By applying the Galerkin procedure, Eqs. (18) and (19) become, in matrix form,

$$[T]\frac{d\{a\}}{dt} + \left[P(\underline{a}^{(n)})\right]\{a\} + \left[P(\underline{a})\right]\{a\}^{(n)} + g\,[S]\{b\} + \left[Q\left(G|u| + q/A\right)^{(o)}\right]\{a\} - \left[P\left(\underline{a}^{(n)}\right)\right]\{a^{(n)}\} = 0, \tag{20}$$

$$[T]\frac{d\{b\}}{dt} + \left[P\left(\underline{a}^{(n)}\right)\right]\{b\} + \left[P(\underline{a})\right]\{b^{(n)}\} + \left[P\left(A^{(o)}/B\right)\right]\{a\} + \left[Q\left(S_o + \frac{\partial A}{\partial x}/B\right)^{(o)}\right]\{a\} - [T]\{q/B\} = 0, \tag{21}$$

in which the matrices $[T]$, $[S]$, $[P]$, and $[Q]$ are defined previously in Eqs. (9)-(12). Eqs. (20) and (21) are coupled, linear ordinary differential equations. At a particular time iterative solutions are obtained until $|\{a\} - \{a^{(n)}\}|$ and $|\{b\} - \{b\}^{(n)}|$ are less than a specified tolerance before further increment of time. Experience suggests that this criterion can usually be met within one or two quasi-linear iterations.

2. Crank-Nicholson Time-differencing Scheme

The Crank-Nicholson scheme is now applied to integrate Eqs. (20) and (21).

Since $$\left[P(\underline{a})\right]\{b\} = \left[P^*(\underline{b})\right]\{a\} \tag{22}$$

where $$\left[P^*(b)\right] = \sum_{j=1}^{m} U_{ijk} b_j$$

Eqs. (20) and (21) can be assembled such that they appear as

$$\left[C\right]\frac{d\{\xi\}}{dt} + \left[D\right]\{\xi\} = \{F\} \tag{23}$$

where the vector $\{\xi\}$ has dimension 2M and $\xi_{2i-1} = a_i$ and $\xi_{2i} = b_i$.

Using a finite-difference expression for $\frac{d}{dt}\{\xi\}$, we write Eq. (23) in the form

$$\left(\left[C\right] + \left[D\right]/2\right)\left(\{\xi\}^{+} - \{\xi\}^{-}\right) = \{F\} - \left[D\right]\{\xi\}^{-}/2 \tag{24}$$

where $\{\xi\} = \{\xi\ (t_o)\}$ and $\{\xi\}^{+} = \{\xi\ (t_o + \Delta t)\}$.

The difference of the present and past $\{\xi\}$, i.e. $\{\xi\}^{+} - \{\xi\}^{-}$, is actually solved to minimize possible round-off errors that could have been incurred in the computations. Because of the properties of the functions $\psi_i(x)$, the coefficient matrix ($[C]$ + $[D]$ /2) is banded and diagonally dominant. An extended Cholesky algorithm (Tewarson, 1973) satisfactorily solves Eq. (24).

In summary, using an implicit time-difference scheme, we have (1) quasi-linearized the nonlinear partial differential equations, (2) applied the Galerkin procedure in the space domain, (3) integrated the resultant ordinary differential equations with respect to time by the Crank-Nicholson finite difference scheme.

III. A Case Study

Three-mile Slough, which is located about 40 miles northeast of San Francisco in the delta region of California's central valley, provides an interesting example of tide-induced, unsteady, open-channel flow. The slough is actually a channel approximately three miles in length connecting the Sacramento and San Joaquin Rivers, Fig. 2.

The long-period tidal waves propagate inland through Golden Gate, San Francisco Bay, San Pablo Bay, Carquinez Strait, Suisan Bay, and on. At the confluence of the San Joaquin River with the Sacramento River near the city of Pittsburgh, the waves divide and continue to propagate upstream in the separate river channels. Because of lesser distance above the confluence and because of greater channel depth, a translatory wave crest passes the Sacramento River end of Three-mile Slough from 30 to 45 minutes before the corresponding wave crest reaches the slough's San Joaquin River end. As a result, Three-mile Slough exhibits continuously and rapidly varying flow through each tidal cycle. Moreover, the direction of flow alternates with the passage of each successive wave. Because of the high degree of unsteadiness and alternating direction of the flow, this tidal reach was deemed desirable for trial evaluation of the discharge computation process.

In 1959, Water Resources Division of the U.S.G.S. conducted an extensive field investigation in this tidal reach. Two tidal gages were installed at the San Joaquin and at the Sacramento River ends to record water levels at 15-minute intervals. A field survey was also conducted to help establish its cross-sectional properties. During the months of July and August, 1959, gates blocked all the diversionary channels, and several sets of discharge measurements were made using current meters. These data were used to evaluate the computational schemes suggested in the present study.

Using the measured stage records at the ends of the Three-mile Slough (See Fig. 2) as inputs, the computations have been carried out by both the predictor-corrector and Crank-Nicholson schemes for several values of Manning coefficient. Figure 3 is a plot of measured and computed discharges obtained by the predictor-corrector scheme for three different Manning values. A Manning value of 0.038 gives a best over-all fit for this scheme. Since the discharge ranges between +35,000 cfs (ft^3/sec) to -35,000 cfs, it is quite likely that the Manning n value should have been treated as a function of the discharge. We have not included this feature in the present study, although implementation of a variable n in the model is plausible. For a Manning coefficient of 0.038, Figure 4 compares the computed discharges for the predictor-corrector and quasi-linearization schemes to those computed by the predictor-corrector scheme with linear basis functions. The predictor-corrector schemes both were run with a 1-minute time-step, and the Crank-Nicholson (quasi-linearization) scheme with a 5-minute time-step. The deviation of the quasi-linearization scheme is attributable to the different manner in which it handles the friction term. For a reach with channel geometry as regular and length as short as Three-mile Slough, there is little difference in the discharges computed using the Hermite and linear basis functions. All of the schemes compute discharges within 5 percent of the measured values.

IV. Discussion

In this study numerical solutions to the governing equation of a tidal reach have been constructed using a Galerkin-finite element approximation in space and finite-difference approximation in time. The computer algorithms have been successfully tested in a case study at Three-mile Slough, California, where a complete reversal of flow takes place in every semi-diurnal tidal cycle. The predictor-corrector

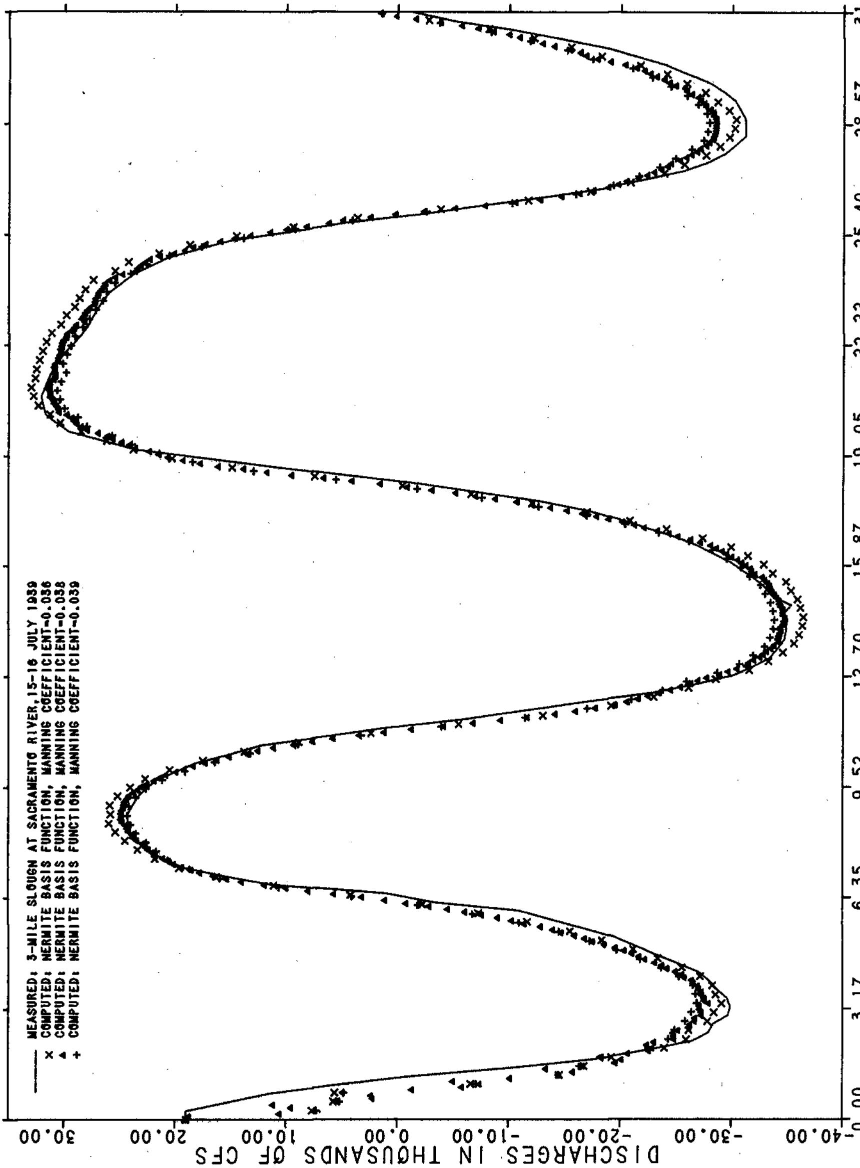

Figure 3. Comparison of the Computed and Measured Discharges at Sacramento River for Various Values of Manning Coefficient

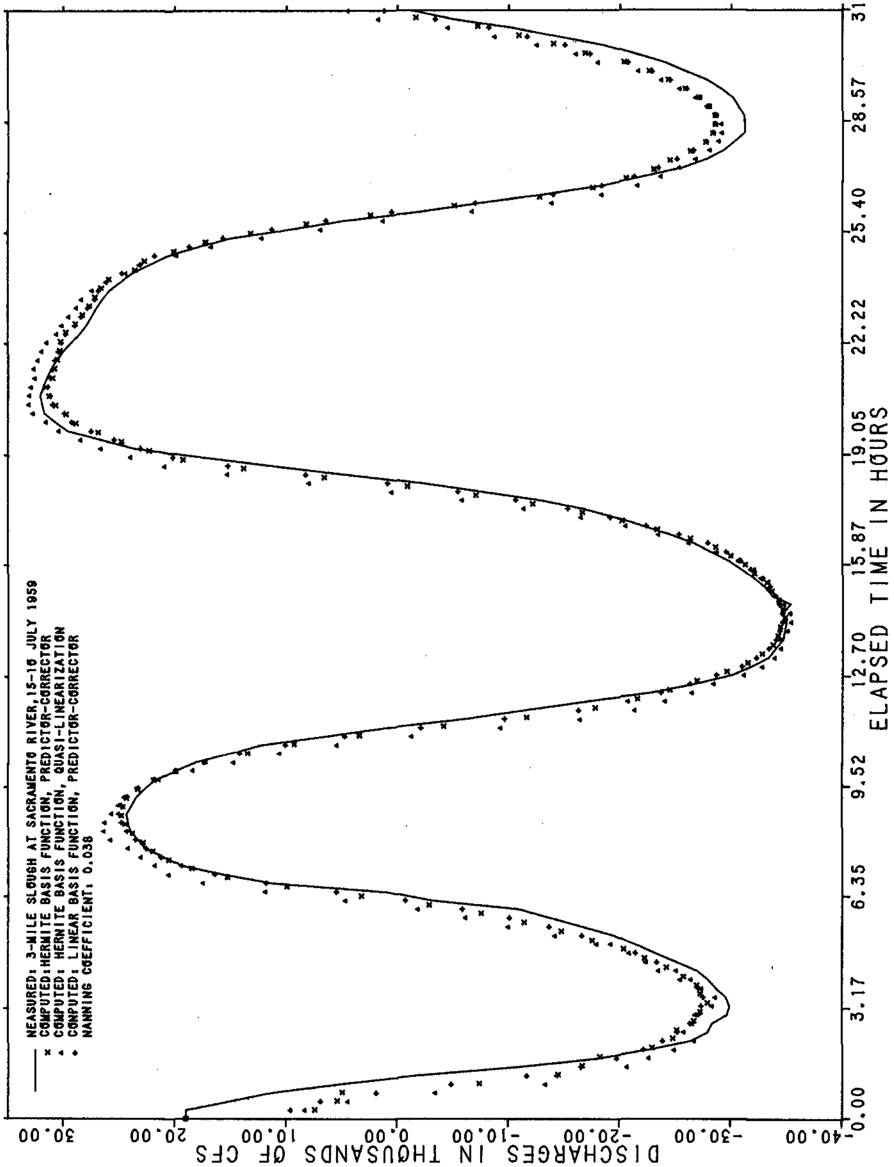

Figure 4. Discharges at Sacramento River Computed by Various Numerical Schemes

solution computes accurate discharges but requires use of the characteristic equations to implement the boundary conditions, and small time-steps to maintain numerical stability. The implicit Crank-Nicholson and quasi-linearization scheme has neither of these requirements. Although it requires longer computer time per time step, it permits the use of larger time steps. The total computer time requirements for the implicit and explicit methods are comparable. Good agreement between the measured and computed discharges suggests further applications of the present model to realistic field problems.

V. References

1. Baltzer, R. A. and Lai, V. C., 1968, Computer simulation of unsteady flow in waterways, Journal of Hydraulic Division, ASCE, Vol. 94, No. HY.4, p. 1083-1117.

2. Bellman, R. E. and Kalaba, R. E., 1965, Quasi-linearization and Nonlinear Boundary-Value Problems, Elsevier, New York

3. Chow, V. T., 1959, Open Channel Hydraulics, McGraw-Hill, New York, 680 p.

4. Cooley, R. L. and Moin, S. A., 1976, Finite Element Solution of Saint-Venant Equations, Journal of Hydraulic Division, ASCE, Vol. 102, No. HY.6, p. 759-775.

5. Dronkers, J. J., 1964, Tidal Computations in Rivers and Coastal Waters, North-Holland Publishing Co., Interscience, Amsterdam, p. 518.

6. Eisenberg, M. A., and Malvern, L. E., 1973, On Finite Element Integration in Natural Coordinates, Int. J. for Num. Meth. in Eng., Vol. 7, No. 4., p. 574-575.

7. Finlayson, B. A., 1972, The method of weighted residuals and variational principles, Academic Press, New York, 412 p.

8. Ralston, A. and Wilf, H. S., 1960, Mathematical Methods for Digital Computers, Wiley, New York, p. 95-109.

9. Smith, L. H., 1975, Finite element solution for one-dimensional unsteady flow in an open channel, (ABS.), Hydr. Eng. for Optional Use of Water Resources, Specialty Conference, ASCE, Seattle, Wash.

10. Stoker, J. J., 1957, Water Waves, Interscience, New York, 567 p.

11. Strang, G. and Fix, G. J., 1973, An Analysis of the Finite Element Method, Prentice-Hall, Englewood Cliffs, N.J.

12. Tewarson, R. P., 1973, Sparse Matrices, Academic Press, New York, 160 p.

13. Wang, H. H., Halpern, P., Douglas, Jr., J., and Dupont, T., 1972, Numerical Solutions of the One-Dimensional Primitive Equations Using Galerkin Approximations with Localized Basis Functions, Mon. Weath. Rev., Vol. 100, No. 10, p. 738-746.

Appendix I. Spatial Integration with Hermite Basis Functions

To facilitate easy application of the Galerkin procedure, we first partition the domain $[0, L]$ into N elements, i.e.,

$$0 = x_o < x_1 < x_2 < \ldots < x_n = L,$$

where the i-th element spans $[x_{i-i}, x_i]$. The local coordinates L_1 and L_2 are introduced such that any point x on the line element $[x_1, x_2]$ can be expressed as

$$x = L_1(x)\, x_1 + L_2(x)\, x_2 \tag{I-1}$$

where

$$L_1(x) = \frac{x_2 - x}{x_2 - x_1}, \quad L_2(x) = \frac{x - x_1}{x_2 - x_1}$$

The functions L_1 and L_2, known as the natural or local coordinates, are simply ratios of length when measured from x_2 and x_1 respectively, and satisfy

$$L_1 + L_2 = 1. \tag{I-2}$$

Utilization of the properties of local coordinates significantly simplifies evaluation of integrals over the elements. General quadratures in terms of the local coordinates can be derived easily (Eisenberg and Malvern, 1973). For one-dimensional problems, we redefine, for the i-th element,

$$L_{i,1}(x) = \frac{x_i - x}{x_i - x_{i-1}}, \quad L_{i,2}(x) = \frac{x - x_{i-1}}{x_i - x_{i-1}}, \tag{I-3}$$

then

$$\int_{x_{i-1}}^{x_i} L_{i,1}^{\alpha}\, L_{i,2}^{\beta}\, dx = \frac{\alpha!\, \beta!\, L_i}{(\alpha + \beta + 1)!}, \text{ where } L_i = x_i - x_{i-1}.$$

The cubic Hermit polynomials can be defined in natural coordinates as

$$\psi_{2i-1}(x) = \begin{cases} -2\,L_{i,2}^3 + 3\,L_{i,2}^2 & \text{if } x_{i-1} \le x \le x_i \\ 2\,L_{i+1,2}^3 - 3\,L_{i+1,2} + 1, & \text{if } x_i \le x \le x_{i+1} \\ 0 & \text{otherwise}, \end{cases} \tag{I-4}$$

$$\psi_{2i}(x) = \begin{cases} L_{i,2}^2\,L_{i,1}\,L_i\,, & \text{if } x_{i-1} \le x \le x_i \\ L_{i+1,1}^2\,L_{i,2}\,L_{i+1}, & \text{if } x_i \le x \le x_{i+1} \\ 0 & \text{otherwise}. \end{cases} \tag{I-5}$$

The functions $\psi_{2i-1}(x)$ and $\psi_{2i}(x)$ are sketched in Fig. 5 for the sub-regions $[x_{i-1}, x_i]$ and $[x_i, x_{i+1}]$, or the i-th and (i+1)-th elements.

Note that

$$\psi_{2i-1}(x_i) = 1\,, \qquad \psi_{2i}(x_i) = 0,$$
$$\frac{d\psi_{2i-1}}{dx}(x_i) = 0\,, \quad \text{and} \quad \frac{d\psi_{2i}}{dx}(x_i) = 1. \tag{I-6}$$

These imply in Eqs. (3) and (4) of section II A that

$$a_{2i-1}(t) = u(x_i,t)\,, \qquad a_{2i}(t) = \left.\frac{\partial u}{\partial x}\right)_{x = x_i},$$
$$b_{2i-1}(t) = Z(x_i,t)\,, \qquad b_{2i}(t) = \left.\frac{\partial Z}{\partial x}\right)_{x = x_i}. \tag{I-7}$$

Thus $\bar{u}$ and $\bar{Z}$ are interpolation expressions for the functions u and Z in terms of their values and spatial gradients at the x_i. The interpolating functions ψ_i constitute a basis for the set of $C^{(1)}$-elements in one-dimensional problems (Strang and Fix, 1973). The numerical solutions are the discrete solutions of velocity and stage at each node, u_i and Z_i and their spatial gradients, $\frac{du_i}{dx}$ and $\frac{dZ_i}{dx}$. Therefore, $C^{(1)}$ elements provide continuous approximate u, z, $\frac{du}{dx}$ and $\frac{dZ}{dx}$ but piecewise continuous second order derivatives.

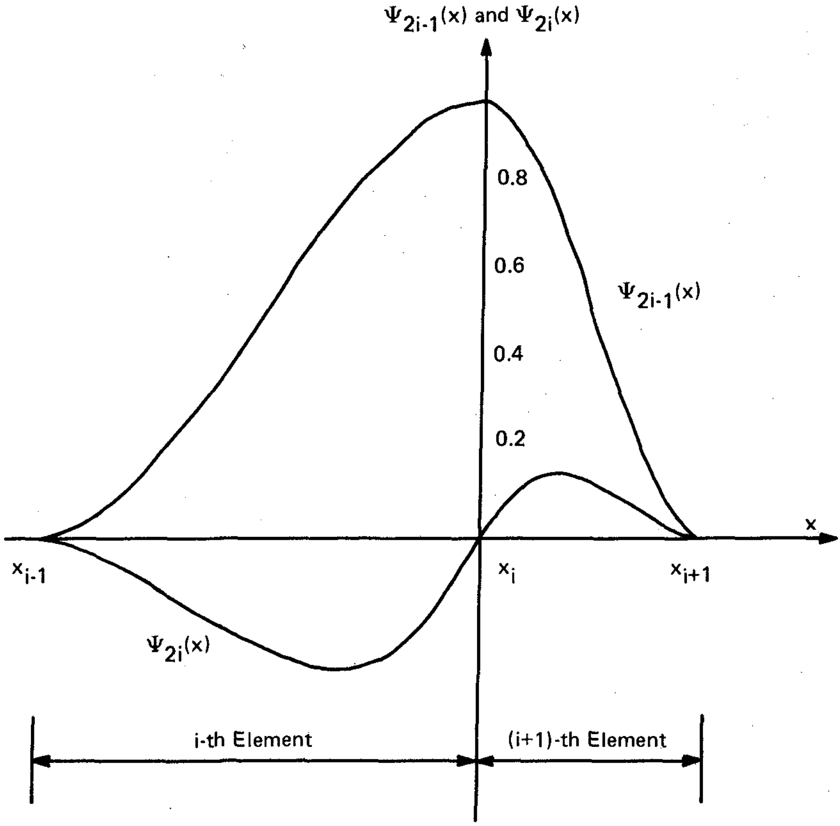

Figure 5. The Cubic Hermite Polynomial Shape Functions for i-th and (i+1)-th Elements

Integrals defining the coefficient matrices, Eqs. (9)-(14), can now be examined. For example,

$$[T] = \int_0^L \psi_i \, \psi_j \, dx = \sum_{k=1}^{n} \int_{x_{k-1}}^{x_k} \psi_i \, \psi_j \, dx. \tag{I-8}$$

Note that unless i, j = 2k - 1, 2k, 2k + 1, or 2k + 2,

$$\int_{x_{k-1}}^{x_k} \psi_i \, \psi_j \, dx = 0.$$

Therefore the elemental contribution to $[T]$ from $[x_{k-1}, x_k]$ can be given as

$$[T]^{(k)} = \frac{L_k}{420} \begin{bmatrix} \frac{156}{L_k} & 22 & \frac{54}{L_k} & -13 \\ 22 & 4\,L_k & 13 & -3\,L_k \\ \frac{54}{L_k} & 13 & \frac{156}{L_k} & -22 \\ -13 & -3\,L_k & -22 & 4\,L_k \end{bmatrix} \tag{I-9}$$

where the first through the fourth column and row represent rows and columns from (2k-1) to (2k+2) in the global (over-all) matrix. This recurrence formula constitutes the basic algorithm of the finite element method. The global matrix $[T]$ is formed by adding the elemental contributions to the proper rows and columns. Likewise, elemental contributions of $[S]^{(k)}$, $[U_{ij}^{(k)}]_1$, $[V_{ij}^{(k)}]_1$ have been calculated and their values are given in Appendix II.

Appendix II. Elemental Contributions of Coefficient Matrices.

$$[S]^{(k)} = \int_{x_{k-1}}^{x_k} \psi_i \frac{d\psi_j}{dx}\, dx = \frac{1}{60}\begin{bmatrix} -30 & -6\ L_k & -30 & 6\ L_k \\ 6\ L_k & 0 & -6\ L_k & L_k^{\ 2} \\ 30 & 6\ L_k & 30 & -6\ L_k \\ -6\ L_k & -L_k & 6\ L_k & 0 \end{bmatrix}.$$

$$\left[U_{ij}^{(k)}\right]_\ell = \int_{x_{k-1}}^{x_k} \psi_i \frac{d\psi_j}{dx} \psi_\ell \, dx, \text{ then}$$

when $\ell = 2k - 1$:

$$\left[U_{ij}^{(k)}\right]_\ell = \frac{1}{840}\begin{bmatrix} -280 & 100\ L_k & 280 & -68\ L_k \\ -50\ L_k & 5\ L_k^2 & 50\ L_k & -11\ L_k^2 \\ -140 & -16\ L_k & 140 & -16\ L_k \\ 34\ L_k & 3\ L_k^2 & -34\ L_k & 5\ L_k^2 \end{bmatrix},$$

when $\ell = 2\ K$:

$$\left[U_{ij}^{(k)}\right]_\ell = \frac{1}{840}\begin{bmatrix} -50\ L_k & 5\ L_k^2 & 50\ L_k & -11\ L_k^2 \\ -10\ L_k^2 & 0 & 10\ L_k^2 & -2\ L_k^3 \\ -34\ L_k & -5\ L_k^2 & 34\ L_k & -3\ L_k^2 \\ 8\ L_k^2 & L_k^3 & -8\ L_k^2 & {}^{3}_{k} \end{bmatrix},$$

when $\ell = 2\ K + 1$

$$\left[U_{ij}^{(k)}\right]_\ell = \frac{1}{840}\begin{bmatrix} -140 & -16\ L_k & 140 & -16\ L_k \\ -34\ L_k & -5\ L_k^2 & 34\ L_k & -3\ L_k^2 \\ -280 & -68\ L_k^2 & 280 & 100\ L_k \\ 50\ L_k & 11\ L_k^2 & -50\ L_k & -5\ L_k^2 \end{bmatrix},$$

$\ell = 2k + 2$

$$\left[U_{ij}^{(k)}\right]_\ell \qquad \begin{bmatrix} 34\ L_k & 3\ L_k^2 & -34\ L_k & 5\ L_k^2 \\ 8\ L_k^2 & L_k^3 & -8\ L_k^2 & L_k^3 \\ 50\ L_k & 11\ L_k^2 & -50\ L_k & -5\ L_k^2 \\ -10\ L_k^2 & -2\ L_k^2 & 10\ L_k^2 & 0 \end{bmatrix}.$$

$$\left[V_{ij}^{(k)}\right]_\ell = \int_{x_{k-1}}^{x_k} \psi_i\ \psi_j\ \psi_\ell\ dx\ ,$$

when $\ell = 2k - 1$:

$$\left[V_{ij}^{(k)}\right]_\ell = \frac{L_k}{2520} \begin{bmatrix} 774 & 97\ L_k & 162 & -43\ L_k \\ 97\ L_k & 16\ L_k^2 & 35\ L_k & -9\ L_k^2 \\ 162 & 35\ L_k & 162 & -35\ L_k \\ -43\ L_k & -9\ L_k^2 & -35\ L_k & 8\ L_k^2 \end{bmatrix},$$

when $\ell = 2k$:

$$\left[V_{ij}^{(k)}\right]_\ell = \frac{L_k}{2520} \begin{bmatrix} 97\ L_k & 16\ L_k^2 & 35\ L_k & -9\ L_k^2 \\ 16\ L_k^2 & 3\ L_k^3 & 8\ L_k^2 & -2\ L_k^3 \\ 35\ L_k & 8\ L_k^2 & 43\ L_k & -9\ L_k^2 \\ -9\ L_k^2 & -2\ L_k^3 & -9\ L_k^2 & 2\ L_k^3 \end{bmatrix},$$

when $\ell = 2k+1$:

$$\left[V_{ij}^{(k)}\right]_{\ell} = \frac{L_k}{2520}\begin{bmatrix} 162 & 35\,L_k & 162 & -35\,L_k \\ 35\,L_k & 8\,L_k^2 & 43\,L_k & -9\,L_k^2 \\ 162 & 43\,L_k & 774 & -97\,L_k \\ -35\,L_k & -9\,L_k^2 & -97\,L_k & 16\,L_k^2 \end{bmatrix},$$

when $= 2k+2$:

$$\left[V_{ij}^{(k)}\right]_{\ell} = \frac{L_k}{2520}\begin{bmatrix} -43\,L_k & -9\,L_k^2 & -35\,L_k & 8\,L_k^2 \\ -9 & -2\,L_k^3 & -9\,L_k^2 & 2\,L_k^3 \\ -35\,L_k & -9\,L_k^2 & -97\,L_k & 16\,L_k^2 \\ 8\,L_k^2 & 2\,L_k^3 & 16\,L_k^2 & -3\,L_k^3 \end{bmatrix}$$